LAWRENCE
LIVERMORE
NATIONAL
LABORATORY

LLNL-JRNL-639918

The Collisionless Magnetoviscous-thermal Instability

T. S. Islam

June 26, 2013

Astrophysical Journal

Disclaimer

LLNL-JRNL-639918

The Collisionless Magnetoviscous-thermal Instability

Tanim Islam

Lawrence Livermore National Laboratory, P. O. Box 808, Livermore, CA 94551-0808

islam5@llnl.gov

Received _____; accepted _____

ABSTRACT

It is likely that nearly all central galactic massive and supermassive black holes are nonradiative: their accretion luminosities are orders of magnitude below what can be explained by efficient black hole accretion within their ambient environments. These objects, of which Sagittarius A* is the best-known example, are also dilute (mildly collisional to highly collisionless) and optically thin. In order for accretion to occur, magnetohydrodynamic instabilities must develop that not only transport angular momentum, but also gravitational energy generated through matter infall, outwards. A class of new magnetohydrodynamical fluid instabilities – the magnetoviscous-thermal instability (MVTI) (Islam 2012) – was found to transport angular momentum and energy along magnetic field lines through large (fluid) viscosities and thermal conductivities. This paper describes the analogue to the MVTI, the collisionless magnetoviscous-thermal instability (CMVTI), that similarly transports energy and angular momentum outwards, expected to be important in describing the flow properties of hot, dilute, and radiatively inefficient accretion flows around black holes. We construct a local equilibrium for MHD stability analysis in this differentially rotating disk. We then find and characterize specific instabilities expected to be important in describing their flow properties, and show their qualitative similarities to instabilities derived using the fluid formalism. We conclude with further work needed in modeling this class of accretion flow.

1. Introduction

Within the recent past, much progress has been made in characterizing the important dynamics of accretion flows. The magnetorotational instability (Velikhov 1959;

Chandrasekhar 1960) has been applied to accretion disks (Balbus & Hawley 1991) and been shown to drive MHD fluid turbulence that can provide an outward angular momentum flux and mass accretion rate consistent with astrophysical observations, as demonstrated in a variety of numerical simulations (Hawley et al. 1996; Wardle 1999; Sano & Stone 2002; de Villiers & Hawley 2003; Fromang et al. 2004). However, there exists observational evidence of hot dilute flows, in accretion about dim mass-starved supermassive black holes, for which the mean free path is of the order of the system scale or larger. Chandra X-ray observations by Baganoff et al. (2003) have resolved the inner 1" around the Sagittarius A central black hole and demonstrated that the ion mean free path at its capture radius is only a few times smaller than the system scale. The unambiguous detection of Faraday rotation in the high- frequency radio emission about Sagittarius A (Aitken et al. 2000; Bower et al. 2003; Marrone et al. 2005) implies that the magnetic field is very easily strong enough to result in a gyrokinetic reduction in plasma dynamics. Estimates of mass accretion from the ambient conditions about this object overestimate its bolometric luminosity by approximately five orders of magnitude over radiatively efficient accretion (Narayan 2002), implying that very little of the gravitational energy produced by mass accretion is radiated. However, recent nonlinear local simulations, with limits on electron pressure anisotropy due to gyrokinetic electron instabilities, show that the nonlinear development of the collisionless MRI can turbulently heat electrons sufficiently to allow these flows to become radiative (Sharma et al. 2007); accretion in collisionless environments, such as those around Sag. A*, may naturally be radiative enough that the accretion rate must remain orders of magnitude below the Bondi rate in order to explain their low luminosity. Regardless of whether this accretion is radiatively inefficient, it is very likely that in the steady state these plasmas are dilute, optically thin, and the bulk of their thermal energy lies with the protons. Furthermore, MHD plasma turbulence that transports energy generated from accretion may play an important role even in high-energy radiative, but collisionless, accretion flows.

The fact that, very plausibly, these systems may be radiatively inefficient points to the fact that these high energy, dilute plasmas are at least partially pressure supported; this is in contrast to a large class of models of radiatively efficient classical accretion disks, in which the accreting disk of matter remains geometrically thin and rotationally supported due to the efficient radiation of energy perpendicular to the disk. Numerical simulations of the MRI in a canonical black hole accretion flow (de Villiers & Hawley 2003; de Villiers et al. 2003) tend to stabilize into thick disks. The large aspect ratio of these disks invites an analysis of these disks with vertical disk structure included, or as a beginning a local analysis in which dynamically important gradients of temperature and pressure govern the nature of local instabilities.

A formulation of magnetized plasma dynamics that is especially well-suited for collisionless or mildly collisional MHD plasma equilibrium and dynamics is that of Kulsrud's drift-kinetic approximation to the Boltzmann equation (Kulsrud 1983, 2005). To lowest order the particle distribution function is characterized by dynamics only along magnetic field lines, MHD conditions of quasi-neutrality with ions and electrons moving together, and conservation of magnetic moment for particle distributions. Furthermore, it is expected that additional dynamics that cannot be modeled through the Kulsrud formalism, such as momentum and energy transfer processes resulting in temperature equilibration or electric resistivity, may not be dynamically important to a first approximation.

For this problem we consider the following hierarchy of scales appropriate to lowest-order gyro kinetic expansion: $1/T < \omega_{pi} \ll \Omega_{ci}$, $1/L < \omega_{pi}/c \ll \rho_i$, where ω_{pi} is the ion plasma frequency, Ω_{ci} is the ion gyrofrequency, ρ_i is the ion gyroperiod, ω_{pi}/c is the inverse ion inertial depth, and L and T are the shortest length and fastest time scales associated with this system. Densities are large enough that Alfvén velocities are smaller than the speed of light, therefore relativistic MHD effects may be ignored. The gravitational acceleration is purely due to that of the central object. We consider a plasma

equilibrium where pressures parallel and perpendicular to the magnetic field are equal, hence the equilibrium particle distribution for electrons and ions has one temperature. We formulate the problem in a cylindrical geometry, where the axis of rotational lies along the vertical axis. $\hat{\boldsymbol{R}}$, $\hat{\boldsymbol{\phi}}$, and $\hat{\boldsymbol{z}}$ are unit vectors in the radial, azimuthal, and vertical directions, respectively.

The organization of this paper is as follows: in §2 we discuss the variables and nomenclature used in this paper; in §3, we use a form of the drift kinetic equation that represents particle dynamics in a co-rotating frame, explicitly state the equilibrium we choose in our local analysis, and include total MHD force balance and MHD induction equations in a co-rotating frame. In §4 we justify and modify turbulent and average wave quantities appropriate to characterize accretion (see, e.g., Balbus & Hawley (1998); Balbus (2004)) in dilute and radiatively inefficient magnetized flows. In §5 we consider the stability of hot dilute rotating plasmas to a new instability, the collisionless analogue to the magnetoviscous-thermal instability (MVTI) (Islam 2012), the collisionless MVTI or CMVTI. We also demonstrate that quadratic estimates of heat fluxes and Reynolds stress are of the right form to drive accretion in this dilute thick flow. In §6 we summarize our main results as well as describe directions for further research.

2. Variables and Nomenclature

Our coordinate system for the rotating disk is a cylindrical system located about the central mass. R is the radial coordinate, ϕ is the azimuthal angle, and z the vertical coordinate aligned along the axis of rotation. $\left(\hat{\boldsymbol{R}}, \hat{\boldsymbol{\phi}}, \hat{\boldsymbol{z}}\right)$ refer to unit vectors in the radial, azimuthal, and vertical directions, respectively. For field variables of temperature T, pressure p, density ρ, electric and magnetic fields $\mathbf{E}$ and $\mathbf{B}$, and pressure p, we use the following notation:

- Equilibrium value of, say density: ρ_0,
- Perturbed density: $\delta\rho$,
- Total density (equilibrium + perturbed): $\rho = \rho_0 + \delta\rho$.

For velocity, we use the following notation:

- Primary equilibrium flow velocity, which is azimuthal: $\mathbf{V}_0 = R\Omega(R)\hat{\boldsymbol{\phi}}$, where $\Omega(R)$ is the orbital angular velocity,
- Perturbed flow velocity: $\delta\mathbf{u}$,
- Total flow velocity: $\mathbf{V} = R\Omega(R)\hat{\boldsymbol{\phi}} + \mathbf{u}$.

Components of an equilibrium vector quantity, such as the radial component of the equilibrium magnetic field, are written as B_{R0}. The radial component of, for instance, the perturbed magnetic field is denoted as δB_R.

In this paper, we consider an electron-ion plasma. In these systems, the ions and electrons are only very weakly coupled collisionally, so the pressure of both species may differ significantly. In an electron-ion plasma, p_i refers to ion pressure, p_e to electron pressure. Quantities such as equilibrium ion pressure will be denoted as p_0, while perturbed species variables such as perturbed ion pressure are denoted as δp_i. Finally, in a collisionless MHD plasma we find it convenient to consider fluid properties, such as parallel $p_\parallel$ and perpendicular $p_\perp$ pressure, that are velocity moments of the particle distribution function. For example, the equilibrium ion parallel pressure is defined as $p_{i\parallel 0}$ and the perturbed ion parallel pressure is $\delta p_{i\parallel}$.

3. The Drift Kinetic And Constituent Equations in Rotating Frame

In this section we state the equations and disk equilibrium used in the eigenmodal analysis and the demonstration of quadratic heat flux of the CMVTI. Without derivation (see, e.g., Hinton & Hazeltine (1976); Sharma et al. (2003); Sharma & Hammett (2006)), the collisionless drift kinetic equation in a rotating frame can be shown to be of the following form,

$$\left(\frac{\partial}{\partial t}+\Omega\frac{\partial}{\partial\phi}\right)(f_sB)+\nabla\cdot\left(\left[v_\parallel\mathbf{b}+\mathbf{u}_\perp\right]f_sB\right)+\frac{\partial}{\partial v_\parallel}\left(f_sB\left[\frac{Z_se}{m_s}E_\parallel+\frac{1}{m_sn_0}\mathbf{b}\cdot\nabla p_{s0}\right]\right)+$$
$$\frac{\partial}{\partial v_\parallel}\left(f_sB\left[-\mathbf{b}\cdot\left(\left[\frac{\partial}{\partial t}+\Omega\frac{\partial}{\partial\phi}\right]\mathbf{u}_\perp+\left[v_\parallel\mathbf{b}+\mathbf{u}_\perp\right]\cdot\nabla\mathbf{u}_\perp\right)+\mu B\nabla\cdot\mathbf{b}+\right.\right. \quad (1)$$
$$\left.\left.2\Omega\hat{\boldsymbol{z}}\cdot(\mathbf{b}\times\mathbf{u})-b_\phi R\left(\mathbf{u}_\perp+v_\parallel\mathbf{b}\right)\cdot\nabla\Omega\right]\right)=0,$$

f_s is the species particle distribution function, and m_s and Z_s is the mass and charge of a particle of species s. $v_\parallel$ is the component of corotating velocity along the magnetic field, and μ is the magnetic moment ($mv_\perp^2/(2B)$). Additional terms appear in the formulation of Eq. (1) that do not appear explicitly in the normal drift-kinetic equation of Kulsrud (1983): non-inertial rotational accelerations along the magnetic field, $2\Omega\hat{\boldsymbol{z}}\cdot(\mathbf{b}\times\mathbf{u})-b_\phi R\left(\mathbf{u}_\perp+v_\parallel\mathbf{b}\right)\cdot\nabla\Omega$, and accelerations along the magnetic field associated with large thermal energies, $1/(m_sn_0)\,\mathbf{b}\cdot\nabla p_{s0}$.

Next, the form of the full MHD force balance and induction equations in a co-rotating frame are given by,

$$\rho\left(\left[\frac{\partial}{\partial t}+\Omega\frac{\partial}{\partial\phi}\right]\mathbf{u}+\mathbf{u}\cdot\nabla\mathbf{u}-2\Omega\mathbf{u}\times\hat{\boldsymbol{z}}+R\mathbf{u}\cdot\nabla\Omega\hat{\boldsymbol{\phi}}\right)=\frac{1}{c}\mathbf{J}\times\mathbf{B}+\frac{n}{n_0}\nabla p-\nabla\cdot\mathbb{P}, \quad (2)$$
$$\frac{\partial\mathbf{B}}{\partial t}=-\mathbf{u}\cdot\nabla\mathbf{B}-\mathbf{B}\left(\nabla\cdot\mathbf{u}\right)+\mathbf{B}\cdot\nabla\mathbf{u}+R\hat{\boldsymbol{\phi}}\mathbf{B}\cdot\nabla\Omega-\Omega\frac{\partial\mathbf{B}}{\partial\phi}. \quad (3)$$

Where $p=p_e+p_i$, $\mathbb{P}=p_\perp\mathbb{I}+\left(p_\parallel-p_\perp\right)\mathbf{bb}$, $p_\parallel=p_{i\parallel}+p_{e\parallel}$, and $p_\perp=p_{i\perp}+p_{e\perp}$. Parallel,

perpendicular, and total pressures are given by their standard forms,

$$p_{s\parallel} = 2\pi \int m_s \left(v_\parallel - u_\parallel\right)^2 f_s \left(B\, d\mu\, dv_\parallel\right), \tag{4}$$

$$p_{s\perp} = 2\pi \int m_s \mu B f_s \left(B\, d\mu\, dv_\parallel\right), \tag{5}$$

$$p_s = \frac{2}{3} p_{s\perp} + \frac{1}{3} p_{s\parallel}. \tag{6}$$

In this paper we analyze the stability and quadratic transport of an equilibrium geometrically thin nonradiative, collisionless disk at its midplane. For simplicity, temperature is independent of height above the disk. To lowest order there is no net current, the plasma velocity is purely azimuthal, and the equilibrium magnetic field is nonradial and axisymmetric. Therefore, the electron and ion pressure and density as a function of vertical coordinate z goes as,

$$n_{i0}, n_{e0}, p_{i0}, p_{e0} \sim \exp\left(-\frac{z^2}{2H^2}\right). \tag{7}$$

The disk scale height H is given by,

$$H^2 = \frac{k_B \left(T_{i0} + T_{e0}\right)}{\left(m_i + m_e\right)\Omega^2}. \tag{8}$$

The equilibrium solution to Eqs (1) is,

$$f_{s0} = \frac{n_0(z=0)}{\left(2\pi k_B T_{s0}/m_s\right)^{3/2}} \exp\left(-\frac{z^2}{2H^2} - \frac{m_s v_\parallel^2}{2k_B T_{s0}} - \frac{m_s \mu B}{k_B T_{s0}}\right). \tag{9}$$

The equilibrium magnetic field $\mathbf{B}_0$ and its vector normal $\mathbf{b}_0$ are,

$$\mathbf{B}_0 = B_0 \left(\hat{\boldsymbol{\phi}} \sin\chi + \hat{\boldsymbol{z}} \cos\chi\right), \tag{10}$$

$$\mathbf{b}_0 = \hat{\boldsymbol{\phi}} \sin\chi + \hat{\boldsymbol{z}} \cos\chi. \tag{11}$$

Global equilibria of axisymmetric, and at least partially rotationally supported, plasmas (Hinton & Hazeltine 1976; Bisnovatyi-Kogan & Seidov 1985; Ogilvie 1997) are characterized by a complicated global geometry due to the requirements of centrifugal force

balance and equilibrium along axisymmetric magnetic surfaces. Local analysis away from the disk midplane, or global analysis of the longer wavelength CMVTI in a high-aspect ratio collisionless accretion disk, is beyond the scope of this paper.

4. Turbulent and Wave Fluxes For Dilute Rotating Plasmas

The evolution equation for the total energy within a disk, using methods outlined in Balbus & Hawley (1998), is given by the following (see, e.g., Sharma & Hammett (2006)):

$$\left(\frac{\partial}{\partial t}+\Omega\frac{\partial}{\partial\phi}\right)\left(\frac{1}{2}\rho u^2+\frac{3}{2}p+\frac{B^2}{8\pi}\right)+\nabla\cdot\mathcal{F}_E-\rho\mathbf{u}\cdot\frac{1}{\rho_0}\nabla p_0= -\frac{\partial\Omega}{\partial\ln R}W_{R\phi}-R\frac{\partial\Omega}{\partial z}W_{z\phi}-Q_{-}. \tag{12}$$

A fuller derivation of Eq. (12) can be found in, e.g., Islam (2007). $\mathcal{F}_E$ is the heat flux arising from local fluctuations, $W_{R\phi}$ is the azimuthal stress, $W_{z\phi}$ is the vertical-azimuthal stress, Q_{-} is a radiative loss term. One may look to Sharma & Hammett (2006); Islam (2007), for fuller derivations of the energy balance term including the pressure expression term. In the context of disk accretion theory, the above expresses the fact that energy is generated by azimuthal stresses that couple to the free energy available from radial and vertical angular velocity gradients. This energy can then be accounted for in various ways: in a classical accretion disk, the energy flux is almost wholly radiated away; in a geometrically thick accretion disk, turbulent heat fluxes are large enough to transport at least some of this viscously generated energy (Balbus & Hawley 1998; Balbus 2003). Even in collisionless accretion, turbulent energy generation may heat electrons until they become radiatively efficient at locally dissipating energy (Sharma et al. 2007). However, in nonradiative flows (Narayan et al. 1998), viscously generated energy must be carried away by a turbulent heat flux (Balbus 2004).

The energy flux is given by,

$$\mathcal{F}_E = \mathbf{u}\left(\frac{1}{2}\rho u^2 + \frac{5}{2}p\right) + \frac{1}{4\pi}\mathbf{B}\times(\mathbf{u}\times\mathbf{B}) + \mathbf{b}q + p_v\left([\mathbf{u}\cdot\mathbf{b}]\,\mathbf{b} - \frac{1}{3}\mathbf{u}\right). \tag{13}$$

The first term in $\mathcal{F}_E$ corresponds to flux of gas kinetic energy, the second to the enthalpy, and the third term corresponds to Poynting MHD flux. The heat flux $q = q_i + q_e$ and pressure difference $p_v = p_{vi} + p_{ve}$ are defined in, e.g., Chang & Callen (1992a,b) in the context of heat flux expressions to model collisionless transport due to specific instabilities into a fluid formalism, and shown here,

$$\begin{aligned} q_s &= \frac{1}{2}q_{s\parallel} + q_{s\perp}, \\ q_{s\parallel} &= 2\pi\int m_s\left(v_\parallel - u_\parallel\right)^3\left(B\,d\mu\,dv_\parallel\right)f_s, \\ q_{s\perp} &= 2\pi\int m_s\left(v_\parallel - u_\parallel\right)(\mu B)\left(B\,d\mu, dv_\parallel\right)f_s. \end{aligned} \tag{14}$$

$$p_{sv} = p_{s\parallel} - p_{s\perp}. \tag{15}$$

The fourth and fifth terms of Eq.(13) correspond to contributions due to heat fluxes along the magnetic field and the viscous stress. $W_{R\phi}$ and $W_{z\phi}$ are given by,

$$W_{R\phi} = \rho u_R u_\phi - \frac{B_R B_\phi}{4\pi} + p_v b_R b_\phi, \tag{16}$$

$$W_{z\phi} = \rho u_z u_\phi - \frac{B_z B_\phi}{4\pi} + p_v b_z b_\phi. \tag{17}$$

The angular momentum flux can be derived from MHD force balance and continuity, and for an accretion disk is given by (Balbus & Hawley 1998; Islam 2007),

$$\begin{aligned} &\left(\frac{\partial}{\partial t} + \Omega\frac{\partial}{\partial\phi}\right)\left(\rho R\left[u_\phi + R\Omega\right]\right) + \\ &\nabla\cdot R\left(\rho\mathbf{u}\left[u_\phi + R\Omega\right] - \frac{B_\phi\mathbf{B}}{4\pi} + p_v b_\phi\mathbf{b} + \left[p_\perp + \frac{B^2}{8\pi}\right]\hat{\boldsymbol{\phi}}\right) = 0. \end{aligned} \tag{18}$$

To understand how local fluctuations about mean quantities of the form $A = A_0 + \delta A$, whether waves or turbulence, can tap into sources of energy within this rotating system, it is easiest to consider the truncated dynamics of this system by averaging vertically and

azimuthally. Define the following averaged quantity:

$$\langle A \rangle = \frac{1}{H} \int_0^{2\pi} \int_{z=-\infty}^{z=\infty} A \, dz \, d\phi, \tag{19}$$

and consider fluctuations which spatially average to zero, i.e. $\langle \delta A \rangle = 0$. Contributions of fluctuations appear at second order. Since in equilibrium $\mathbf{u}_0 = \mathbf{0}$, $p_{\parallel 0} = p_{\perp 0} = p_0$, $q_0 = 0$, and $q_{v,0} = 0$, the energy and angular momentum equations are,

$$\frac{\partial \langle L \rangle}{\partial t} + \frac{1}{R} \frac{\partial}{\partial R} \left(R^3 \Omega \langle \rho u_R \rangle + R \langle W_{R\phi} \rangle \right) = 0, \tag{20}$$

$$\frac{\partial \langle \mathcal{E} \rangle}{\partial t} + \frac{1}{R} \frac{\partial}{\partial R} R \langle \mathcal{F}_{ER} \rangle - \langle \rho u_R \rangle \frac{1}{\rho_0} \frac{\partial p_0}{\partial R} = - \frac{\partial \Omega}{\partial \ln R} \langle W_{R\phi} \rangle - Q_-. \tag{21}$$

We have ignored the flux of gas kinetic energy, that appears at third order in fluctuating quantities, and the Poynting flux, which is subdominant to the other terms in the energy flux. We have taken $W_{z\phi}$ to be an even function of height. From Eq. (11), the equilibrium azimuthal component of the magnetic normal vector is $\cos \chi$.

$$\langle L \rangle = \langle \rho R \left(u_\phi + R\Omega \right) \rangle, \tag{22}$$

$$\langle \mathcal{E} \rangle = \left\langle \frac{1}{2} \rho u^2 + \frac{1}{2} p_\parallel + p_\perp + \frac{B^2}{8\pi} \right\rangle, \tag{23}$$

$$\langle W_{R\phi} \rangle = \left\langle \rho_0 \delta u_R \delta u_\phi - \frac{\delta B_R \delta B_\phi}{4\pi} + \delta p_v \delta b_R \sin \chi \right\rangle, \tag{24}$$

$$\langle F_{ER} \rangle = \frac{5}{2} \rho_0 \langle \delta u_R \delta \theta \rangle + \langle \delta q \delta b_R \rangle - \frac{1}{3} \langle \delta p_v \delta u_R \rangle. \tag{25}$$

Note that the radial mass flux term $\langle \rho u_R \rangle = \langle \delta \rho \delta u_R \rangle + \rho_0 u_{R2}$, where u_{R2} is a second order steady bulk radial flow of matter with magnitude of order $|\delta \rho / \rho_0|^2$; as noted by Balbus (2003), in a steady-state geometrically thin disk, the net radial matter flux has a magnitude given by $|\langle \rho u_R \rangle| \sim \rho \left| \langle \mathbf{u} \rangle^2 \right| / (R\Omega)$.

5. Stability Analysis And Quadratic Heat Fluxes

The discussion of the CMVTI is divided into the following subsections. §5.1 and 5.2 describe the eigenmodal equations, and collisionless pressure expressions, used to derive the

full dispersion relation for the CMVTI, which is not shown in this work. In the limit of zero equilibrium pressure and temperature gradients, the CMVTI reduces to the collisionless MRI. §5.3 estimates quadratic modal expressions for heat flux and Reynolds stress from the CMVTI. We find it useful to use the following variables and scalings:

$$\begin{aligned}
\theta_0 &= \frac{k_B T_0}{m_i} \\
v_A^2 &= \frac{B_0^2}{4\pi\rho_0} \\
x &= k_\parallel v_A/\Omega \\
\hat{\mathbf{k}} &= \mathbf{k} v_A/\Omega \\
\gamma &= \Gamma/\Omega \\
\alpha_P &= -\left(\theta_0^{1/2}/\Omega\right)\frac{\partial \ln p_0}{\partial R} \\
\alpha_T &= -\left(\theta_0^{1/2}/\Omega\right)\frac{\partial \ln T_0}{\partial R} \\
\beta &= \theta_0/v_A^2.
\end{aligned} \tag{26}$$

Our expression for the Alfvén speed v_A differs by a factor of $\sqrt{2}$ from the standard definition. We also explore the stability of stratified media that are convectively stable, hence one in which $\alpha_S < 0$ or equivalently $\alpha_T < \frac{2}{5}\alpha_P$. All plots of dispersion relations, heat fluxes, and Reynolds stresses use a plasma equilibrium with $\chi = \pi/4$ (equal equilibrium toroidal and vertical magnetic field components), plasma $\beta = 10^2$, Keplerian rotation profile $\Omega \propto R^{-3/2}$, and purely vertical wavenumbers.

5.1. Perturbed Axisymmetric Distribution Function at the Mid-plane

Here we consider an equilibrium density and temperature distribution given in §2. Assume axisymmetric perturbations to equilibrium quantities of the form $\delta a \propto \exp\left(ik_R R + ik_Z z + \Gamma t\right)$, and define $k_\parallel = \mathbf{k}\cdot\mathbf{b}_0$. Eq. (1) then reduces to the following form for ions and electrons, where we assume equal scale heights of radial and vertical ion

and electron temperature gradients:

$$\delta f_i/f_{i0} = \frac{m_i v_\parallel}{k_B T_{i0}} \left(\frac{-ik_\parallel \mu \delta B + e\delta E_\parallel/m_i}{\Gamma + ik_\parallel v_\parallel} - \frac{(2\Omega + \Omega' R)\,\Gamma + ik_\parallel v_\parallel \Omega' R}{ik_\parallel \left(\Gamma + ik_\parallel v_\parallel\right)} \bar{B}_R \sin\chi \right) - \frac{\bar{B}_R}{ik_\parallel} \left(\frac{\partial \ln n_0}{\partial R} - \frac{3}{2}\frac{\partial \ln T_0}{\partial R} + \left(\frac{m_i \mu B_0}{k_B T_{i0}} + \frac{m_i v_\parallel^2}{2k_B T_{i0}} \right) \frac{\partial \ln T_0}{\partial R} \right) + \frac{\bar{B}_R v_\parallel \partial \ln p_0/\partial R}{\Gamma + ik_\parallel v_\parallel}, \tag{27}$$

$$\delta f_e/f_{e0} = \frac{m_e v_\parallel}{k_B T_{e0}} \left(\frac{-ik_\parallel \mu \delta B - e\delta E_\parallel/m_e}{\Gamma + ik_\parallel v_\parallel} - \frac{(2\Omega + \Omega' R)\,\Gamma + ik_\parallel v_\parallel \Omega' R}{ik_\parallel \left(\Gamma + ik_\parallel v_\parallel\right)} \bar{B}_R \sin\chi \right) - \frac{\bar{B}_R}{ik_\parallel} \left(\frac{\partial \ln n_0}{\partial R} - \frac{3}{2}\frac{\partial \ln T_0}{\partial R} + \left(\frac{m_e \mu B_0}{k_B T_{e0}} + \frac{m_e v_\parallel^2}{2k_B T_{e0}} \right) \frac{\partial \ln T_0}{\partial R} \right) + \frac{\bar{B}_R v_\parallel \partial \ln p_0/\partial R}{\Gamma + ik_\parallel v_\parallel}. \tag{28}$$

Terms with Ω arise due to the fact that the plasma is rotating; terms with equilibrium gradients of temperature, density, or pressure may drive convective and free energy gradient instabilities. $\delta E_\parallel$ is the electric field that ensures quasineutrality, i.e. $\int \delta f_i^0 B\, d\mu = \int \delta f_e^0 B\, d\mu$. One can demonstrate that in the limit of dominating ion thermal energy $T_{i0} \gg T_{e0}$ that the electric field $\delta E_\parallel$ and electron dynamic terms (such as $\delta p_{e\perp,\parallel}$) become unimportant in describing the plasma dynamics. This is the simplification employed by Quataert et al. (2002) and Sharma et al. (2003). However, with equilibrium electron temperatures up to one-tenth that of the ion temperatures, as implied by local nonlinear simulations of the collisionless MRI (Sharma et al. 2007), the CMVTI dispersion relation is not substantially altered. Fig. (1) shows that the dispersion relation of the CMVTI is not significantly different between cases where the electron temperature is negligible ($T_{e0} = 10^{-2} T_{i0}$) and where the electron temperature equals the ion temperature.

Using the induction equation Eq. (3) and the continuity equation, the total force balance equation, Eq. (2), is represented by the following in terms of Eq. (26):

$$\gamma^2 \bar{\mathbf{B}} - \gamma^2 \mathbf{b}_0 \left(\frac{\delta\rho}{\rho} - \frac{\alpha_P - \alpha_T}{ix\beta^{1/2}} \bar{B}_R \right) + 2\frac{d\ln\Omega}{d\ln R} \bar{B}_R \hat{\boldsymbol{R}} + 2\gamma \sin\chi \left(\frac{\delta\rho}{\rho} - \frac{\alpha_P - \alpha_T}{ix\beta^{1/2}} \bar{B}_R \right) \hat{\boldsymbol{R}} + 2\gamma \hat{\boldsymbol{z}} \times \bar{\mathbf{B}} = \hat{\mathbf{k}} x\beta \frac{\delta p_\perp}{p_0} + x^2 \beta \frac{\delta p_\parallel - \delta p_\perp}{p_0} \mathbf{b}_0 - ix\beta^{1/2} \alpha_P \frac{\delta\rho}{\rho} \hat{\boldsymbol{R}} - x^2 \bar{\mathbf{B}} + \hat{\mathbf{k}} x \frac{\delta B}{B}, \tag{29}$$

$\delta B/B = \bar{B}_\phi \sin\chi - (k_R/k_Z)\, \bar{B}_R \cos\chi$, $\delta p_\parallel = \delta p_{i\parallel} + \delta p_{e\parallel}$, and $\delta p_\perp = \delta p_{i\perp} + \delta p_{e\perp}$. Contributions due to $\delta\rho/\rho - (\alpha_P - \alpha_T) \,/\, \left(ix\beta^{1/2}\right) \bar{B}_R$ arise from finite plasma compressibility; in the

Boussinesq limit these terms are set to zero. The eigenvalue problem consists of three equations for solving $\bar{B}_R$, $\bar{B}_\phi$, and $\delta\rho/\rho$: radial force balance, azimuthal force balance, and force balance along $\mathbf{b}_0$.

$$\left(\gamma^2 + x^2\left[1 + \frac{k_R^2}{k_Z^2}\right] + 2\frac{d\ln\Omega}{d\ln R} - 2\gamma\sin\chi\frac{\alpha_P - \alpha_T}{ix\beta^{1/2}}\right)\bar{B}_R - \left(2\gamma + x^2\tan\chi\frac{k_R}{k_Z}\right)\bar{B}_\phi + \frac{\delta\rho}{\rho}\left(2\gamma\sin\chi + ix\beta^{1/2}\alpha_P\right) = \frac{k_R}{k_Z\cos\chi}x^2\beta\frac{\delta p_\perp}{p_0}, \tag{30}$$

$$\left(\gamma^2\sin\chi\frac{\alpha_P - \alpha_T}{ix\beta^{1/2}} + 2\gamma\right)\bar{B}_R + \left(\gamma^2 + x^2\right)\bar{B}_\phi - \gamma^2\sin\chi\frac{\delta\rho}{\rho} = x^2\beta\frac{\delta p_\parallel - \delta p_\perp}{p_0}\sin\chi, \tag{31}$$

$$\bar{B}_R\left(\gamma^2\frac{\alpha_P - \alpha_T}{ix\beta^{1/2}} - \gamma^2\frac{k_R}{k_Z}\cos\chi + 2\gamma\sin\chi\right) + \gamma^2\sin\chi\bar{B}_\phi - \gamma^2\frac{\delta\rho}{\rho} = x^2\beta\frac{\delta p_\parallel}{p_0}, \tag{32}$$

$\delta p_\perp$ and $\delta p_\parallel$ are linear functions of $\bar{B}_R$, $\bar{B}_\phi$, and $\delta\rho/\rho$. In subsequent subsections we explore the dispersion relation associated with the rotational magnetothermal and magnetoviscous instabilities. We work in the limit of small electron thermal energies. Therefore, subsequent expressions for perturbed and equilibrium pressure will refer to the ionic component (e.g., $\delta p_{i,\perp} \to \delta p_\perp$, $p_{i0} \to p_0$, $p_{i0} \to p_0$, $T_{i0} \to T_i$).

5.2. Expressions For Perturbed Pressure

In this section we derive expressions for the perturbed parallel and perpendicular pressures, used in closing the eigenmodal equations for the CMVTI (Eqs. [30, 31, 32]). From Eq. (27), expressions for perturbed parallel and perpendicular pressure can be simplified into a linear combination of density, $\delta B/B$, and $\bar{B}_R$,

$$\frac{\delta p_\perp}{p_0} = \frac{\delta\rho}{\rho} - \frac{\delta B}{B}\left(R\left(i\zeta\right) - 1\right) + \frac{\bar{B}_R}{ik_\parallel}\left(\frac{\partial\ln n_0}{\partial R} - \frac{\partial\ln p_0}{\partial R}\right), \tag{33}$$

$$\frac{\delta p_\parallel}{p_0} = \left(\frac{1 - 2\zeta^2 R\left(i\zeta\right)}{R\left(i\zeta\right)}\right)\frac{\delta\rho}{\rho} - \left(\frac{1 - \left[1 + 2\zeta^2\right]R\left(i\zeta\right)}{R\left(i\zeta\right)}\right)\frac{\delta B}{B} + \frac{\bar{B}_R}{ik_\parallel}\left(\frac{1 - 2\zeta^2 R\left(i\zeta\right)}{R\left(i\zeta\right)} \times \frac{\partial\ln n_0}{\partial R} - \frac{\partial\ln p_0}{\partial R}\right). \tag{34}$$

$\zeta = \Gamma / \left(k_\parallel \theta_0 \sqrt{2}\right)$ and $R\left(\zeta\right)$ is the plasma response function,

$$R\left(\zeta\right) = \frac{1}{\sqrt{\pi}} \int_{-\infty}^{\infty} \frac{x e^{-x^2}}{x - \zeta} \, dx. \tag{35}$$

Since the phase velocity of the modes are at best of order the sound speed, i.e. $|\zeta| \lesssim 1$, these perturbations are not adiabatic and the opposite, slow wave ($|\zeta| \ll 1$) limit, holds for most unstable wavenumbers. The plasma response function in the slow wave limit is,

$$R\left(i\zeta\right) = 1 - \zeta\sqrt{\pi} + \mathcal{O}\left(\zeta^2\right). \tag{36}$$

Expressions for perturbed pressure reduce to the following, to first order in ζ:

$$\frac{\delta p_\parallel}{p_0} \rightarrow \frac{\delta\rho}{\rho} + \sqrt{\pi}\zeta\frac{\delta B}{B} - \xi_R \frac{\partial \ln T_0}{\partial R}, \tag{37}$$

$$\frac{\delta p_\perp}{p_0} \rightarrow \frac{\delta\rho}{\rho} - \sqrt{\pi}\zeta\frac{\delta B}{B} + \xi_R \left(3\frac{\partial \ln n_0}{\partial R} - \frac{\partial \ln p_0}{\partial R}\right). \tag{38}$$

From the radial component of Eq. (3), $\bar{B}_R = i k_\parallel \xi_R$, where ξ_R is the radial fluid displacement. Dispersion relations for the CMVTI are displayed in Fig. (2). One feature of the plasma response via the CMVTI is that of relatively strong collisionless Barnes damping of magnetohydrodynamic modes along the magnetic fields for long wavelength modes $k_\parallel < \Omega/\theta_0^{1/2}$, such that at these wavenumbers the phase velocity remains of the order of the sound speed. This feature has been noted in previous studies of the collisionless MRI (Quataert et al. 2002; Sharma et al. 2003). This damping has the effect of suppressing pressure variations for sufficiently small wavelengths. As the equilibrium plasma β decreases to order 1 and smaller the effects of anisotropic pressure become insignificant over much of the range of unstable wavenumbers. Dispersion relations for the CMVTI are similar to the MVTI (Islam 2012). The range of unstable wavenumbers match between fluid and collisionless analogues:

$$0 \leq k^2 v_A^2 / \Omega \leq 2 \left|\frac{d \ln \Omega}{d \ln R}\right| + \alpha_P \alpha_T. \tag{39}$$

Instead of collisionless damping in the case of the instabilities analyzed within this paper, in fluid treatments it is finite (but dynamically important) viscosity and thermal conductivity

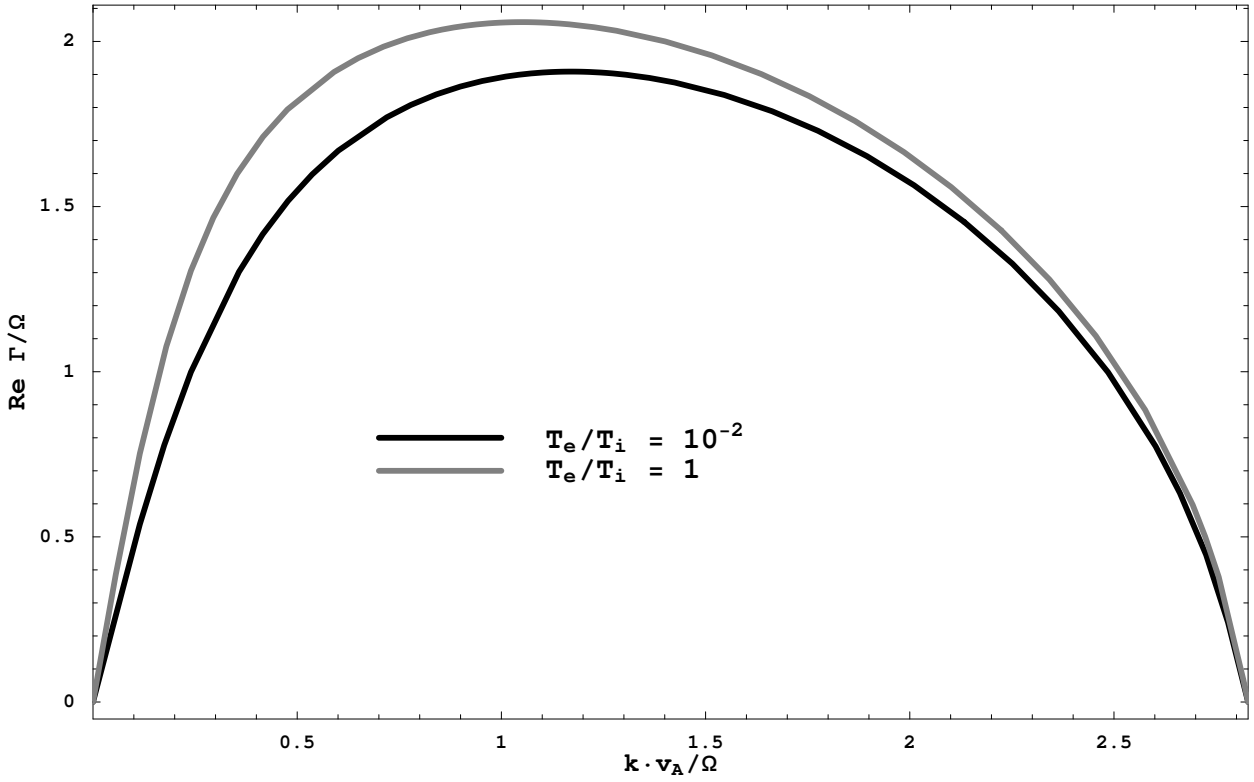

Fig. 1.— Plot of the real part of the growth rate of the CMVTI, for the case where the ion temperature is much larger than the electron temperature $T_{i0}/T_{e0} = 10^2$, and the case where they are equal. $\alpha_P = 5$, and $\alpha_T = 2$ – marginal convective stability. This figure, and a more comprehensive plasma response incorporating electron pressure dynamics and finite equilibrium electron temperature, is taken from Islam (2007).

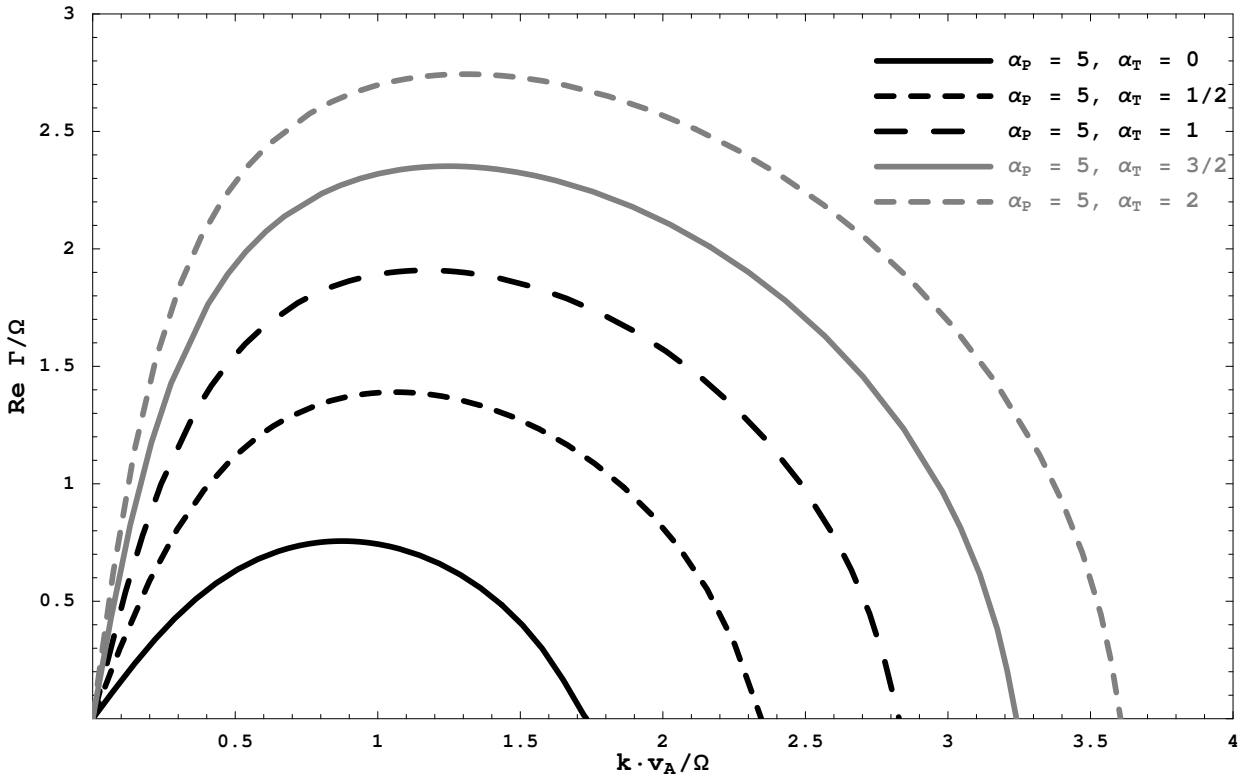

Fig. 2.— Plot of the real part of the growth rate for the CMVTI and different equilibrium radial temperature gradients. Here $\alpha_P = 5$ and different $\alpha_T = 0$, such that $0 < \alpha_T < \frac{2}{5}\alpha_P$, so that the plasma remains convectively stable.

that plays this role. Fig. 1 from Islam (2012), showing the real part of the dispersion relation for the MVTI for a dynamically important viscous diffusion coefficient, realistic Prandtl number, for a range of convectively stable equilibria. Efficient viscosity and

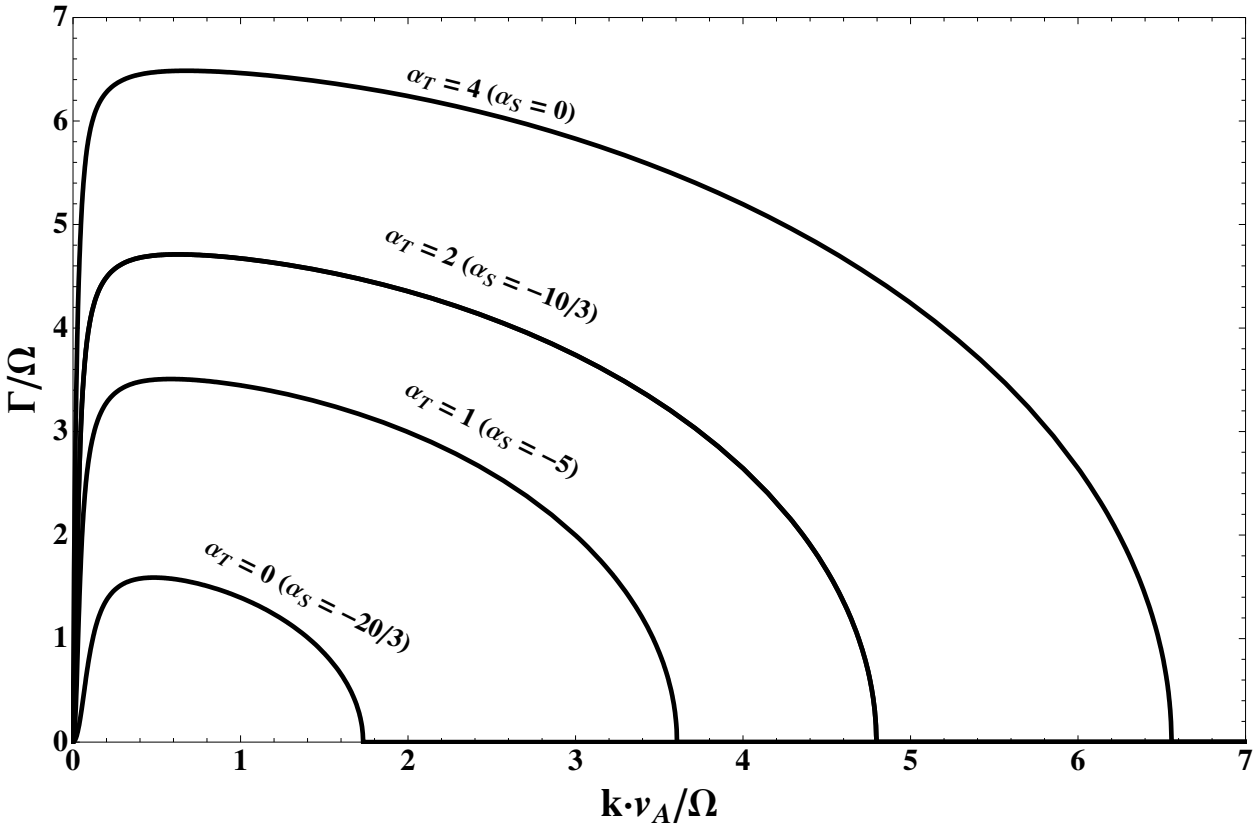

Fig. 3.— Plot of the real portion of the growth rate for th MVTI various α_T. $\alpha_P = 10$, viscous diffusion coefficient $\nu\Omega/v_A^2 = 10^2$, Prandtl number Pr $= 1/101$, and $\alpha_S = 5\alpha_T/3 - 2\alpha_P/3$. Rollover occurs at wavenumbers $k \sim \sqrt{\Omega/\nu} \ll \Omega/v_A$.

thermal diffusivity dissipates the MVTI at wavelengths such that $\nu k^2 \lesssim \Omega$, where ν is a viscous diffusion coefficient along magnetic field lines (Islam & Balbus 2005; Islam 2012). Fluid simulations that model collisionless damping as a form of fluid transport (Sharma & Hammett 2006; Sharma et al. 2007), do so with heat fluxes whose thermal diffusion coefficients are on the order of θ_0/Ω.

5.3. Quadratic Fluxes

Here, we determine the normalized quadratic heat flux, Eq. (25), and the radial azimuthal stress, Eq. (24), associated with a given mode of purely vertical wavenumber k_Z. We normalize these fluxes as a function of fixed Lagrangian radial displacement $\xi_R = \delta u_R/\Gamma$. From Eq. (27), we have the following expressions for $\delta u_\parallel$, $\delta q_\parallel$, and $\delta q_\perp$.

$$\frac{\delta u_\parallel}{\theta_0^{1/2}} = -i\zeta\sqrt{2}R\left(i\zeta\right)\left(\frac{\delta B}{B} - \frac{2\Omega\Gamma}{k_\parallel^2\theta_0}\bar{B}_R\sin\chi + \frac{i\bar{B}_R}{k_\parallel}\left(\frac{\partial \ln p_{i0}}{\partial R}\right)\right) + \frac{i\bar{B}_R}{k_\parallel}\sin\chi\Omega' R, \tag{40}$$

$$\frac{\delta q_\parallel}{p_0\theta_0^{1/2}} = \left(i\zeta\sqrt{2}\left(\frac{\delta B}{B}\right) - \frac{\bar{B}_R}{k_\parallel}\left(\frac{\partial \ln p_0}{\partial R}\right)\zeta\sqrt{2} - \frac{\Omega\zeta^2}{k_\parallel\theta_0^{1/2}}i\bar{B}_R\cos\chi\right)\left(\left[2\zeta^2+3\right]R\left(i\zeta\right) - 1\right), \tag{41}$$

$$\frac{\delta q_\perp}{p_0\theta_0^{1/2}} = -i\zeta\sqrt{2}\left(\frac{\delta B}{B}\right)R\left(i\zeta\right). \tag{42}$$

Expressions for the heat flux and radial-azimuthal stress for these axisymmetric modes at the disk midplane are given by the following:

$$W_{R\phi} = \mathrm{Re}\left(\rho_0\delta u_R^*\delta u_\phi - v_A^2\bar{B}_R^*\bar{B}_\phi + \sin\chi\bar{B}_R^*\delta p_v\right), \tag{43}$$

$$F_{ER} = \mathrm{Re}\left(\frac{5}{2}\delta u_R^*\delta\theta - \delta q\bar{B}_R^* - \frac{1}{3}\delta p_v\bar{B}_R^*\right). \tag{44}$$

One can employ expressions for the total pressure (Eq. [6]), pressure difference (Eq. [15]), and total heat flux (Eq. [14]) with expressions for the perturbed pressures (Eqs. [33] and [34]) and heat fluxes given (Eqs. [41] and [42]). The form of the relative perturbed density and toroidal magnetic field $\delta\rho/\rho$ and $\bar{B}_\phi$ are described in the eigenvalue equations (Eqs. [30], [31], and [32]). Using variable scalings as given by Eq. (26), expressions for δu_R, $\bar{B}_R$, $\bar{B}_\phi$,

δu_ϕ, δp_v, $\delta\theta$, and δq in terms of ξ_R are,

$$\delta u_R = \gamma\left(\Omega\xi_R\right), \tag{45}$$

$$\bar{B}_R = ix\left(\frac{\Omega}{v_A}\xi_R\right), \tag{46}$$

$$\bar{B}_\phi = -\frac{2\gamma\left(\cos^2\chi + R\left(\frac{i\gamma}{x\sqrt{2\beta}}\sin^2\chi\right)\right) - ix\beta^{1/2}\alpha_P\sin\chi\left[R\left(\frac{i\gamma}{x\sqrt{2\beta}}\right)-1\right]}{\gamma^2\left(\cos^2\chi + R\left(\frac{i\gamma}{x\sqrt{2\beta}}\right)\sin^2\chi\right) + x^2 - 2x^2\beta\sin^2\chi\left[\left(1+\frac{\gamma^2}{2x^2\beta}\right)R\left(\frac{i\gamma}{x\sqrt{2\beta}}\right)-1\right]}\times \tag{47}$$
$$ix\left(\frac{\Omega}{v_A}\xi_R\right),$$

$$\begin{aligned}\delta u_\phi =& \frac{\gamma}{ix}v_A\bar{B}_\phi\left(\cos^2\chi + R\left(\frac{i\gamma}{x\sqrt{2\beta}}\right)b_{\phi 0}^2\right) + \\ & \left(\Omega\xi_R\right)\left(\left|\frac{d\ln\Omega}{d\ln R}\right| - \sin\chi\left[\frac{2\gamma^2}{x^2\beta}\sin\chi + i\alpha_P\frac{\gamma}{x\beta^{1/2}}\right]R\left(\frac{i\gamma}{x\sqrt{2\beta}}\right)\right),\end{aligned} \tag{48}$$

$$\begin{aligned}\delta p_v =& \left(p_0 H^{-1}\xi_R\right)\left(\left[\frac{\gamma^2}{x^2\beta}-1\right]R\left(\frac{i\gamma}{x\sqrt{2\beta}}\right)+1\right) + \\ & 2\left(p_0\bar{B}_\phi\sin\chi - i\beta^{-1}\frac{\gamma}{x}p_0\xi_R\frac{\Omega}{v_A}\right)\left(\left[1+\frac{\gamma^2}{2x^2\beta}\right]R\left(\frac{i\gamma}{x\sqrt{2\beta}}\right)-1\right),\end{aligned} \tag{49}$$

$$\begin{aligned}\frac{\delta\theta}{\theta_0} =& \frac{\delta p}{p_0} - \frac{\delta\rho}{\rho} = \left(\xi_R H^{-1}\right)\left(\alpha_T + \alpha_P\left(\left[\frac{5}{3}+\frac{\gamma^2}{3x^2\beta}\right]R\left(\frac{i\gamma}{x\sqrt{2\beta}}\right)-\frac{5}{3}\right)\right) + \\ & \frac{1}{3}\bar{B}_\phi\sin\chi\left(\left[\frac{\gamma^2}{2x^2\beta}-1\right]R\left(\frac{i\gamma}{x\sqrt{2\beta}}\right)+1\right) - \\ & \frac{2}{3}i\beta^{-1}\frac{\gamma}{x}\sin\chi\left(\frac{\Omega}{v_A}\xi_R\right)\left(\left[1+\frac{\gamma^2}{x^2\beta}\right]R\left(\frac{i\gamma}{x\sqrt{2\beta}}\right)-1\right),\end{aligned} \tag{50}$$

$$\begin{aligned}\delta q =& \left(p_0\Omega\xi_R\right)\sin\chi\left(i\alpha_P\frac{\gamma}{x\beta^{1/2}}+\frac{2\gamma^2}{x^2\beta}\right)\left(\left[\frac{3}{2}+\frac{\gamma^2}{2x^2\beta}\right]R\left(\frac{i\gamma}{x\sqrt{2\beta}}\right)-\frac{1}{2}\right) + \\ & i\left(p_0\theta_0^{1/2}\bar{B}_\phi\right)\frac{\gamma}{2x\beta^{1/2}}\sin\chi\left(\left[1+\frac{\gamma^2}{x^2\beta}\right]R\left(\frac{i\gamma}{x\sqrt{2\beta}}\right)-1\right).\end{aligned} \tag{51}$$

The azimuthal stress is normalized in units of $\rho_0\Omega^2\left|\xi_R\right|^2$ and the heat flux in terms of $\rho_0\theta_0^{1/2}\Omega^2\left|\xi_R\right|^2 \equiv p_0\Omega H^{-1}\left|\xi_R\right|^2$. The relatively involved quadratic expressions for angular momentum and heat flux are not shown. In Figs. (4) and (5) are plots of the heat flux and azimuthal stress for the CMVTI for different $0 < \alpha_T < \frac{2}{5}\alpha_P$.

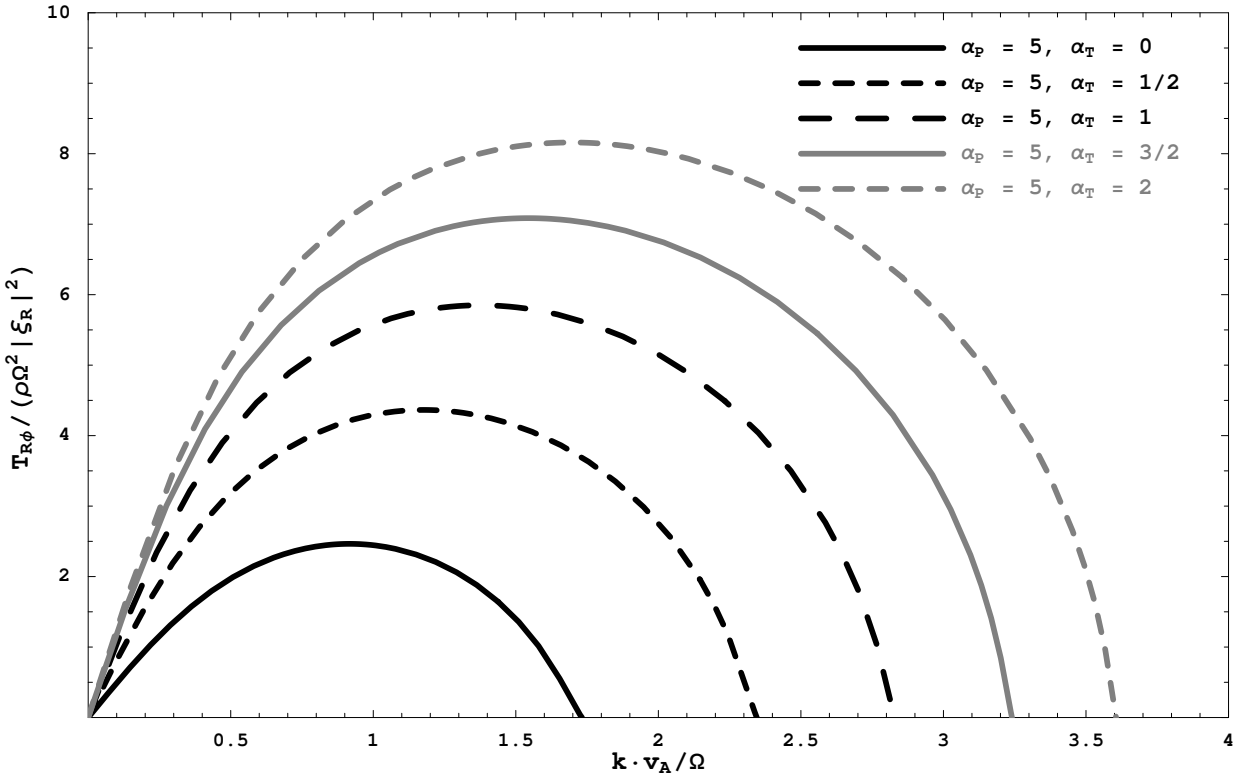

Fig. 4.— Outwards normalized azimuthal stress for the CMVTI and various convectively stable equilibrium profiles with $\alpha_P = 5$ and $0 \leq \alpha_T \leq 2$.

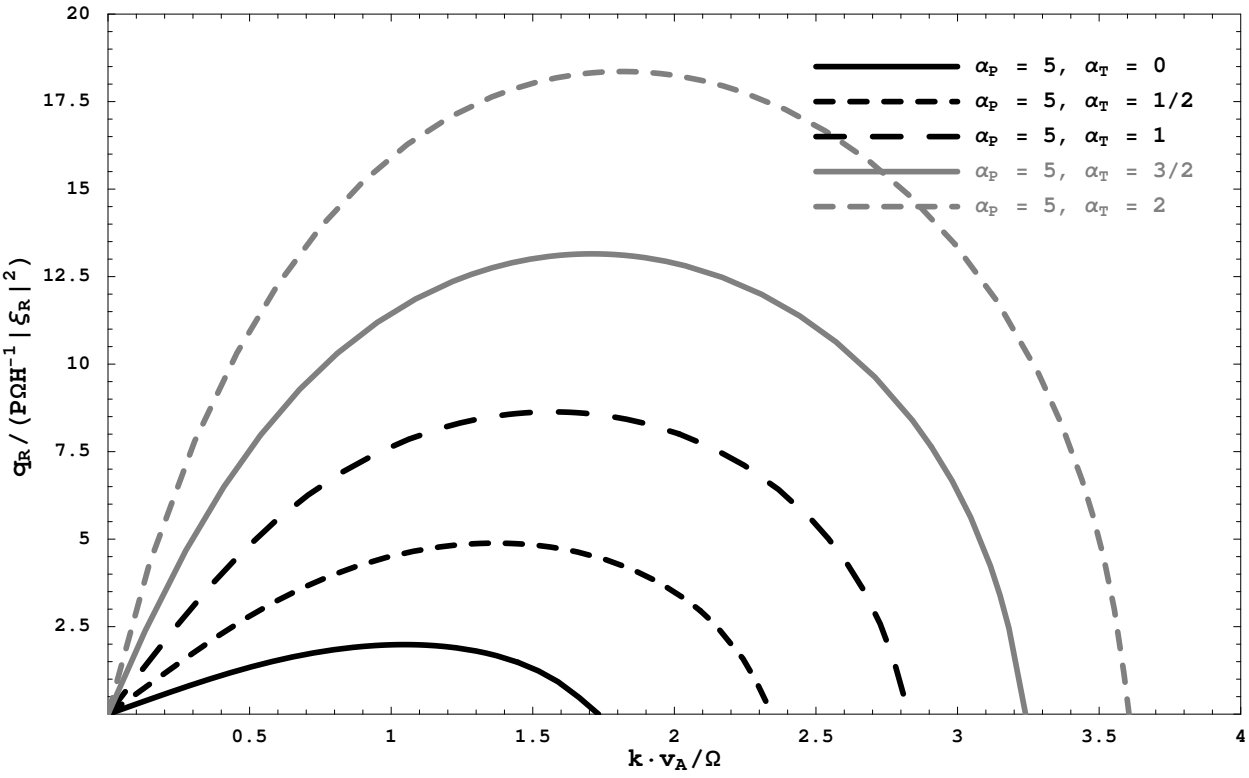

Fig. 5.— Same as Fig. (4), except for quadratic heat flux.

One can easily demonstrate, by setting $\alpha_P = \alpha_T = 0$, that the heat flux for the collisionless MRI is zero. There are no equilibrium radial gradients of temperature or density, the growth rate is purely real, so that for a given mode the temperature and viscous pressure perturbations are out of phase with the perturbed radial velocity, and the perturbed heat flux is out of phase with the perturbed radial magnetic field. The salient features of these instabilities is that they produce the right type of azimuthal stress that can drive accretion. The general sense of the Reynolds stress is outwards for all unstable wavenumbers for the CMVTI; however, Islam (2012) demonstrates that the MVTI can have a generally small range of small wavenumbers for even an unstable Keplerian rotational profile in which the azimuthal stress is negative. Finally, even in the absence of rotational shear $\Omega' R = 0$ the effects of a heat flux can also transport angular momentum outwards; this is demonstrated in Fig. (6). Surprisingly, the CMVTI, even in the absence of differential rotation, is more effective at transporting angular momentum outwards than the MVTI. For comparison, Fig. (7) reproduces Fig. 7 from Islam (2012), and demonstrates that for a substantial portion of unstable wavenumbers, the modal MVTI Reynolds stress is inwards rather than outwards. As noted in Islam (2012), in the absence of rotational shear, no energy can be extracted from the flow (see Eq. (21)). Second, the ambiguity of angular transport for the CMVTI is analogous to the MVTI, in that the CMVTI acts as a mechanism to transport thermal energy outwards, largely (and, in the case of rigid rotation, completely) independent of the manner in which it transports angular momentum. A first step to understand the CMVTI would be to explore unambiguous measures of turbulent, saturated angular momentum and heat flux in local simulations that are marginally stable to the CMVTI and MVTI.

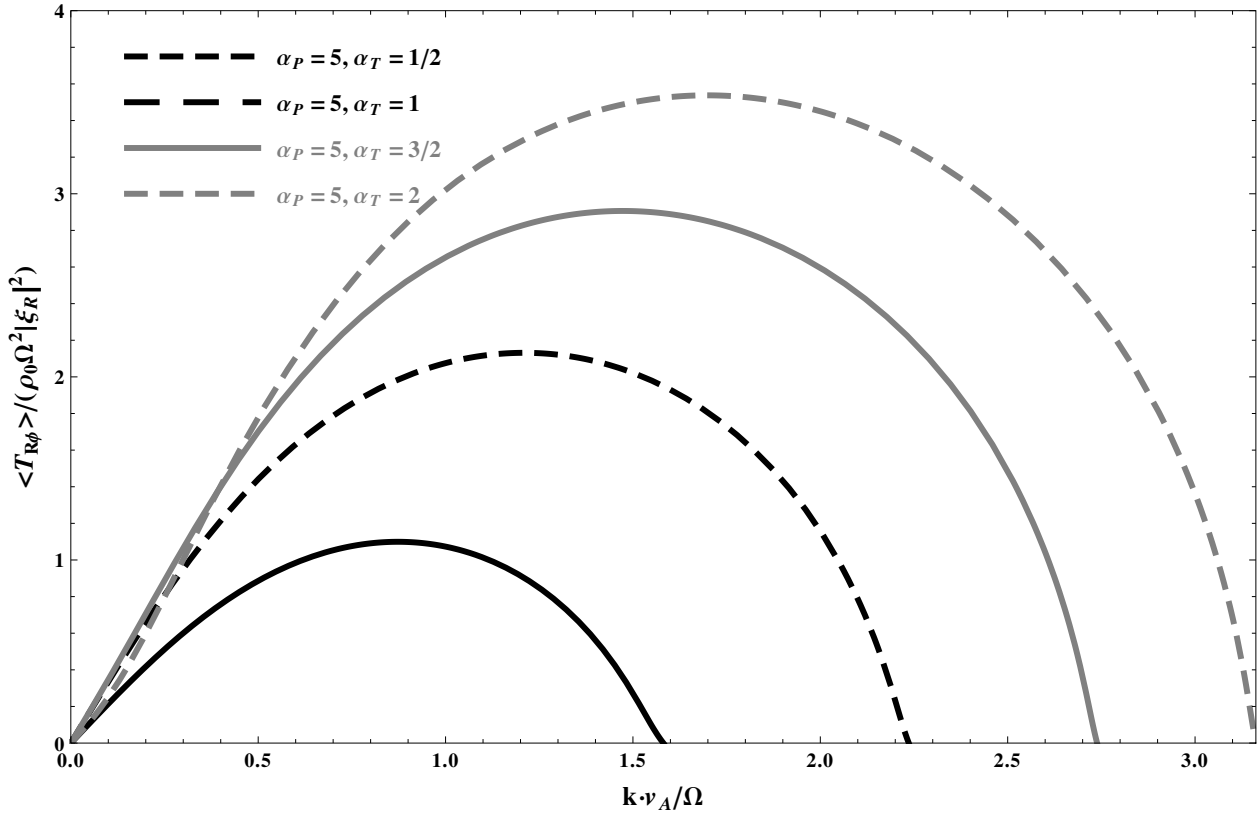

Fig. 6.— Plot of the azimuthal stress for the CMVTI and zero rotational shear, and various convectively stable equilibrium profile.

6. Summary of Results and Further Work

In this paper we have derived the drift kinetic equation explicitly in a rotating frame with possible significant gas pressures and only mild collisionality, with application to hot, dilute, weakly-magnetized (in the sense that magnetic forces are subdominant in equilibrium), at best mildly relativistic systems such as as dim accretion about supermassive black holes. §6.1 describes the main results of this paper. §6.2 elaborates on the main directions for future work.

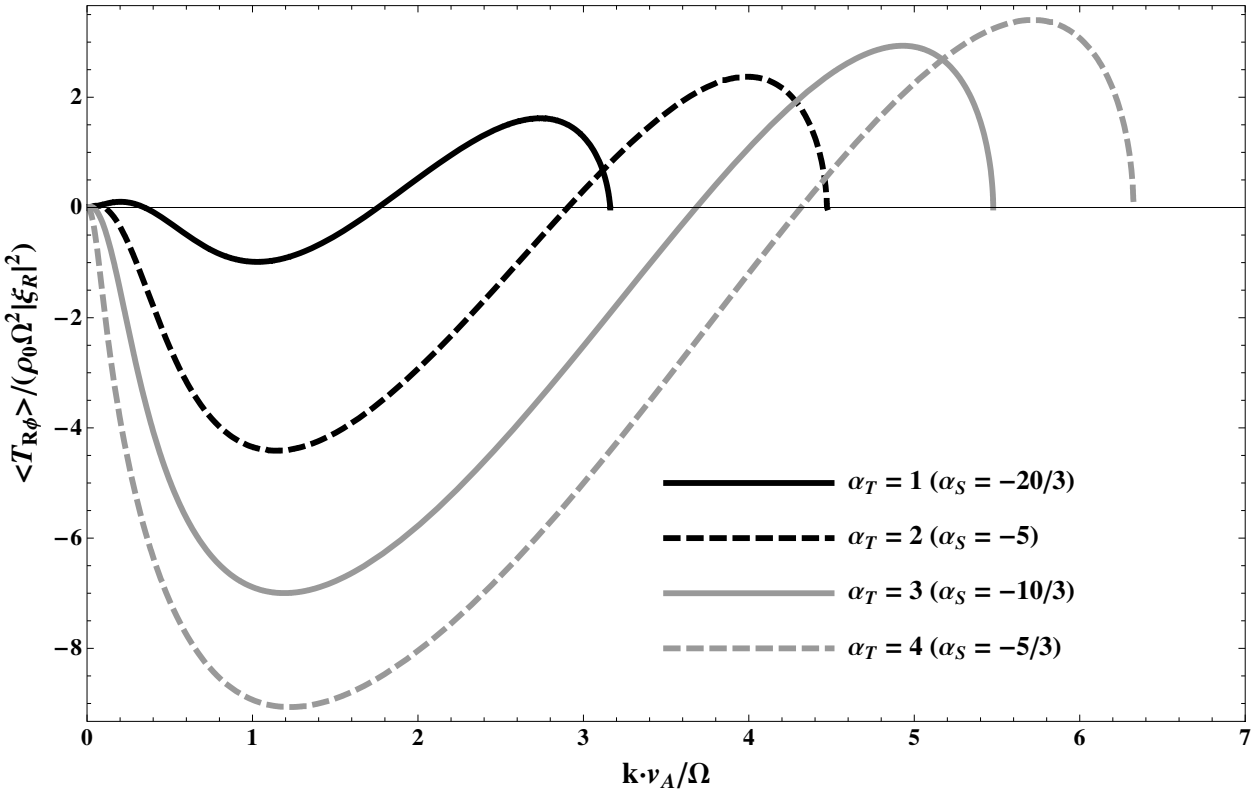

Fig. 7.— Normalized flux $\langle T_{R\phi} \rangle / \left(\rho \Omega^2 \left| \xi_R \right|^2 \right)$ for a rigid rotation profile ($\Omega' R = 0$), and convectively stable equilibria, for the MVTI. $\alpha_S = 5\alpha_T/3 - 2\alpha_P/3$.

6.1. Summary of Results

We see physical terms explicitly associated with disk stratification as well as rotation. We also see that one may rather easily derive modifications of the azimuthal stress and heat flux due to fluctuations or waves in accreting systems (Balbus & Hawley 1998; Balbus 2003) due to dilute plasmas, as demonstrated in §4, in order to characterize how or whether instabilities may create the right type of turbulence that drives accretion.

We have analysed the CMVTI, which have been demonstrated (Islam & Balbus 2005; Islam 2012) from a fluid treatment to destabilize a plasma, through anisotropic viscosities and thermal conductivities, that possesses adverse angular velocity or temperature gradients. We demonstrate the congruence in the dispersion relation for the CMVTI with

the MVTI. Heat fluxes and azimuthal stresses associated with this instability have the right sense (i.e., positive), to drive accretion in fat dilute nonradiative rotating plasmas, and roughly match their respective fluid counterparts. Furthermore, we note that expressions for the normalized pressure and heat gradients, α_P and α_T, go as H/R if we assume that equilibrium temperature and pressure radial scale heights are of order the disk radius. Therefore, we expect only geometrically thick disks to efficiently transport angular momentum in nonradiative accretion flows.

6.2. Future Work

Although we have applied the drift-kinetic equation to a single but important class of instability in Keplerian-like rotating systems, its representation as given in Eq. (1) lends itself to much richer studies of these types of dilute plasmas. Immediate analytic work can enhance our understanding of the stability of a collisionless nonradiative accretion disk to the CMVTI. Due to the requirement of geometrically thick disks to efficiently transport angular momentum without radiative losses, a global stability analysis with realistic disk structure is needed.

Fluid MHD models of local nonlinear evolution in collisionless astrophysical plasmas have employed prescriptions to model collisionless and fast, small-length scale isotropizing phenomena. First, Landau fluid expressions of heat flux and viscosity represent, as practical as is possible, the collisionless momentum and heat transport driven by the instabilities of interest. And second, a hard wall on relative ionic pressure anisotropies reflects observations of marginal pressure anisotropy in the solar wind (Hellinger et al. 2006; Bale et al. 2009), due to unresolvable fast (on the order of the ion gyroperiod) and short wavelength (on the order of the ion gyroradius) instabilities driven by pressure anisotropy. Similar pressure anisotropies are found to develop for the CMVTI, as shown by a more comprehensive

stability analysis Islam (2007). Although these prescriptions have been fruitfully applied to local simulations of the collisionless MRI (Sharma & Hammett 2006; Sharma et al. 2007) and the buoyancy instability (Kunz et al. 2012), a more self-consistent numerical model is desired.

A more productive approach would be to use gyrokinetic or drift-kinetic MHD codes, such as Fokker-Planck (Grandgirard et al. 2006), ionic particle in cell (Kolesnikov et al. 2010; Chen & Parker 2009), or hybrid PIC (Brecht & Thomas 1988) modified such that ions move drift-kinetically, to simulate the dynamics of these plasmas. Recent work in modifying full particle in cell (Riquelme et al. 2012) and 3D hybrid particle in cell (Kunz et al. 2014) for co-rotating local reference frames has found promise in the study of the collisionless differentially rotating plasmas, currently under situations in which the separation of length and time scales with ion gyromotion, disk rotational frequency, and the fastest growing wavelengths of the MRI are not too severe. These numerical models have shown promise in understanding the nonlinear development of initially weak-field (ion gyroradius larger than the wavelength of the fastest growing mode) magnetotational instabilities (Krolik & Zweibel 2006; Ferraro 2007). Enhancements to these codes towards larger spatial and temporal separations between ion gyromotion and the slower, longer scale dynamics of collisionless MHD make them well suited towards understanding the nature of heat flux and angular momentum transport in the CMVTI.

7. Acknowledgements

The author would like to thank the referees, whose input has clarified and focused this paper into a generalization of the MVTI into the collisionless regime, for pointing out a crucial reference (Sharma et al. 2007) demonstrating that the collisionless MRI may heat electrons such that even collisionless accretions flows may become radiative, and for

allowing a further iteration to repair mistakes in content.

Prepared by LLNL under Contract DE-AC52-07NA27344.

REFERENCES

Aitken, D. K., Greaves, J., Chrysostomou, A., Jenness, T., Holland, W. S., Hough, J. H., Pierce-Price, D., & Richer, J. 2000, The Astrophysical Journal Letters, 534, L173

Baganoff, F. K., Maeda, Y., Morris, M. R., Bautz, M. W., Brandt, W. N., Cui, W., Doty, J. P., Feigelson, E. D., Garmire, G. P., & Pravdo, S. H. 2003, The Astrophysical Journal, 591, 891

Balbus, S. A. 2003, Annual Review of Astronomy and Astrophysics, 41, 555

—. 2004, The Astrophysical Journal, 600, 865

Balbus, S. A. & Hawley, J. F. 1991, The Astrophysical Journal, 376, 214

—. 1998, Reviews of Modern Physics, 70, 1

Bale, S., Kasper, J., Howes, G., Quataert, E., Salem, C., & Sundkvist, D. 2009, Physical Review Letters, 103, 211101

Bisnovatyi-Kogan, G. S. & Seidov, Z. F. 1985, Astrophysics and Space Science, 115, 275

Bower, G., Wright, M. C. H., Falcke, H., & Backer, D. 2003, The Astrophysical Journal, 588, 331

Brecht, S. H. & Thomas, V. A. 1988, Computer Physics Communications, 48, 135

Chandrasekhar, S. 1960, Proceedings of the National Academy of Sciences, 46, 253

Chang, Z. & Callen, J. D. 1992a, Physics of Fluids B, 4, 1167

—. 1992b, Physics of Fluids B, 4, 1182

Chen, Y. & Parker, S. E. 2009, Physics of Plasmas, 16, 052305

de Villiers, J.-P. & Hawley, J. F. 2003, The Astrophysical Journal, 592, 1060

de Villiers, J.-P., Hawley, J. F., & Krolik, J. 2003, The Astrophysical Journal, 599, 1238

Ferraro, N. M. 2007, The Astrophysical Journal, 662, 512

Fromang, S., de Villiers, J.-P., & Balbus, S. A. 2004, Astrophysics and Space Science, 292, 439

Grandgirard, V., Brunetti, M., Bertrand, P., Besse, N., Garbet, X., Ghendrih, P., Manfredi, G., Sarazin, Y., Sauter, O., Sonnendrücker, E., Vaclavik, J., & Villard, L. 2006, Journal of Computational Physics, 217, 395

Hawley, J. F., Gammie, C. F., & Balbus, S. A. 1996, The Astrophysical Journal, 464, 690

Hellinger, P., Trávníček, P., Kasper, J. C., & Lazarus, A. J. 2006, Geophysical Research Letters, 33, 09101

Hinton, F. L. & Hazeltine, R. D. 1976, Reviews of Modern Physics, 48, 239

Islam, T. 2007, PhD thesis, University of Virginia

—. 2012, The Astrophysical Journal, 746, 8

Islam, T. & Balbus, S. A. 2005, The Astrophysical Journal, 633, 328

Kolesnikov, R. A., Wang, W. X., Hinton, F. L., Rewoldt, G., & Tang, W. M. 2010, Physics of Plasmas, 17, 2506

Krolik, J. H. & Zweibel, E. G. 2006, The Astrophysical Journal, 644, 651

Kulsrud, R. M. 1983, in Basic Plasma Physics: Selected Chapters, Handbook of Plasma Physics, Volume 1, ed. A. A. Galeev & R. N. Sudan, 1–+

Kulsrud, R. M. 2005, Plasma Physics for Astrophysics, Princeton Series in Astrophysics (Princeton, NJ: Princeton University Press)

Kunz, M. W., Bogdanović, T., Reynolds, C. S., & Stone, J. M. 2012, The Astrophysical Journal, 754, 122

Kunz, M. W., Stone, J. M., & Bai, X. N. 2014, Journal of Computational Physics

Marrone, D. P., Moran, J. M., Zhao, J. H., & Rao, R. 2005, The Astrophysical Journal, 640, 308

Narayan, R. 2002, in Lighthouses of the Universe: The Most Luminous Celestial Objects and Their Use for Cosmology: Proceedings of the MPA/ESO/MPE/USM Joint Astronomy Conference Held in Garching, Harvard-Smithsonian Center for Astrophysics, 60 Garden Street, Cambridge, MA 02138, USA, 405

Narayan, R., Mahadevan, R., Grindlay, J. E., Popham, R. G., & Gammie, C. F. 1998, The Astrophysical Journal, 492, 554

Ogilvie, G. I. 1997, Monthly Notices of the Royal Astronomical Society, 288, 63

Quataert, E., Dorland, W. D., & Hammett, G. W. 2002, The Astrophysical Journal, 577, 524

Riquelme, M. A., Quataert, E., Sharma, P., & Spitkovsky, A. 2012, The Astrophysical Journal, 755, 50

Sano, T. & Stone, J. M. 2002, The Astrophysical Journal, 570, 314

Sharma, P. & Hammett, G. W. 2006, PhD thesis, Princeton Univ., Washington, DC

Sharma, P., Hammett, G. W., & Quataert, E. 2003, The Astrophysical Journal, 596, 1121

Sharma, P., Quataert, E., & Stone, J. M. 2007, The Astrophysical Journal, 671, 1696

Velikhov, E. P. 1959, Zhur Eksptl' i Teoret Fiz, 36, 1398

Wardle, M. 1999, Monthly Notices of the Royal Astronomical Society, 307, 849

This manuscript was prepared with the AAS LaTeX macros v5.2.